Tectonophysics 457 (2008) 197–208

Contents lists available at ScienceDirect

Tectonophysics

journal homepage: www.elsevier.com/locate/tecto

# Enhanced intraplate seismicity along continental margins: Some causes and consequences

Mike Sandiford [a,*], David Lundbek Egholm [b]

[a] School of Earth Sciences, Melbourne University, Victoria, 3010, Australia
[b] Department of Earth Sciences, University of Aarhus, Aarhus, Denmark

ARTICLE INFO

*Article history:*
Received 11 June 2007
Received in revised form 5 June 2008
Accepted 7 June 2008
Available online 14 June 2008

*Keywords:*
Intraplate seismicity
Passive margins
Australia
Structural reactivation
*In situ* stress

ABSTRACT

In Australia, much of the seismic activity is restricted to zones up to several hundred kilometres wide inboard of continental margins at high angle to the trend in maximum horizontal compression ($S_{Hmax}$). Intriguingly, along the margin-side of one such zone, a near optimally oriented, crustal-scale structure – the Darling Fault – has no recorded historical seismicity. To explain these enigmatic features we explore how the compositional and thermal structuring of continental passive margins may lead to variations in mechanical response to imposed forcing using forward modelling. We show how lateral heat flow across such margins can produce increases in Moho temperatures by several 10s of degrees relative to the continental interior extending up to 200 km inboard of the ocean–continent transition, provided the step in thermal lithosphere thickness into the continent is greater than 30 km. For smaller lithospheric steps Moho temperatures beneath continental margins will be cooler than beneath interiors. Our mechanical models show that such thermal effects can elevate strain rates along the margin by several factors relative to continental interiors, when subject to far-field forcing. In the shallow seismogenic-realm, the strain-rate maximum is concentrated at around 100–150 km inboard of the ocean to continent lithospheric step, providing a plausible explanation for the pattern of seismicity observed in some of Australia's marginal seismic zones. This interpretation requires that strength changes associated with Moho temperature variations of several 10s of degrees are sufficient to override the reactivation potential of near optimally oriented crustal-penetrative structures, with thermal processes providing an important "switch" controlling reactivation potential of existing structures. It also provides an insight into the mechanism of formation of continental ribbons during rifting of thermally mature margins.



## 1. Introduction

Intraplate seismicity accounts for only about 5% of the Earth's seismic moment release, with much of this occurring in zones of distributed deformation bordering active plate convergence zones (Johnston et al., 1994). For example, in central Asia distributed deformation can clearly be related to the convergence between the Indo-Australian and Asian plates. In comparison, the controls on the distribution of intraplate earthquakes in stable continental regions (SCR), far from active plate boundaries, is far less well understood. While SCR quakes only account for ~0.5% of the seismic moment release, they tend to be shallow and often in regions characterised by relatively low attenuation, so their effects can be serious (Zoback et al., 1999). The significant, but poorly understood, hazard of SCR quakes is well illustrated by the 1989 $M_w$ 5.6 Newcastle event in Australia that resulted in 13 deaths and ~A$4 billion damage. Prior to this earthquake, there was little expectation of it happening, and we still have only a vague understanding of the future damaging earthquake likelihood, and associated hazard, in this region (e.g. Sandiford, 2003).

While the relative infrequency of SCR events prohibits robust quantification, the available data suggest that the seismic moment release rate of the Australian continent is several times the SCR background rate, ranking behind India as one of the most active of stable continental interiors (Table 1, Johnston et al., 1994). A number of lines of evidence suggest relatively high levels of SCR seismicity in both Australia and India is associated with relatively high levels of intraplate stress throughout the Indo-Australian plate (IAP). For example, the central Indian Ocean is the only intraplate region within an old ocean basin with significant seismic moment release, to the extent in fact that some suggest the IAP has either been, or is in the process of, dismembering into as many as three separate plates (Deplus, 2001; DeMets et al., 2005). The initiation of this central Indian Ocean deformation is dated to around 8 Ma (Krishna et al., 2001), with the incipient fragmentation of the IAP argued to be a response to propagation of stress from distant collisional plate boundaries (Molnar et al., 1993; Sandiford et al., 2005). Such a

* Corresponding author.
*E-mail address:* mikes@unimelb.edu.au (M. Sandiford).

0040-1951/$ – see front matter © 2008 Published by Elsevier B.V.
doi:10.1016/j.tecto.2008.06.004

**Table 1**
Estimates of seismic moment release rate of various stable continental regions after Johnston et al. (1994)

| SCR region | Seismic moment (dyn-cm/year per $10^5$ km$^2$) | Seismic strain rate (year$^{-1}$) | Percent of India |
|---|---|---|---|
| India | $3.3\times10^{23}$ | $25\times10^{11}$ | |
| China | $1.2\times10^{23}$ | $8.9\times10^{11}$ | 36% |
| North America | $1.1\times10^{23}$ | $8.0\times10^{11}$ | 32% |
| Australia | $8.9\times10^{22}$ | $6.7\times10^{11}$ | 27% |
| Africa | $4.0\times10^{22}$ | $3.0\times10^{11}$ | 12% |
| Europe | $2.5\times10^{22}$ | $1.9\times10^{11}$ | 8% |
| South America | $1.2\times10^{22}$ | $8.7\times10^{10}$ | 3.5% |
| Asia | $8.0\times10^{20}$ | $6.1\times10^{10}$ | 0.25% |
| Antarctica | $1.9\times10^{20}$ | $1.4\times10^{10}$ | 0.05% |

mechanism requires propagation of high levels of stress across the neighbouring continental realms of both India and Australia.

As a fast moving plate (5–6.5 cm/year), currently involved in a number of collisional-orogens along its leading edge in the Himalaya, Papua New Guinea and Timor, the IAP has been subject to complex, rapidly evolving, boundary conditions over the last few tens of million years. The impact of the leading-edge "collisions" can be inferred from the pattern of *in situ* stress through the Australian continent (Coblentz et al., 1995; Hillis and Reynolds, 2000; Reynolds et al., 2002), and implicates plate boundary forcing as a critical control on the intraplate stress field along with intraplate variations in density (Coblentz and Sandiford, 1994). A specific example of plate boundary forcing in controlling the *in situ* stress field occurs in southeast Australia where an apparent increase in the tectonic activity at 5–10 Ma correlates with changes in plate motion and coupling between the Australian and Pacific plates that initiated the Southern Alpine orogenic system in New Zealand in the late Miocene (Sandiford, 2003; Sandiford et al., 2004b). Plate-scale stress modelling that shows how plate boundary forcing from the vicinity of the Southern Alps of New Zealand, the Puysegur Trench and the Macquarie Ridge provides a compelling explanation for the unusual orientation of the stress field within southeast Australia where the characteristic trend of $S_{HMax}$ forms a high angle to the absolute plate velocity (Fig. 1). Fault slip rates deduced from the neotectonic record in southeast Australia (Quigley et al., 2006) are consistent with the present-day seismic moment release rate of order $10^{-17}$–$10^{-16}$ s$^{-1}$ (Sandiford et al., 2004b; Leonard, 2008; Braun et al., in press), and further corroborate the notion that distant plate boundary forcing provides a significant sources of the stress associated with Australian seismicity (Sandiford et al., 2004b).

While ongoing seismicity within Australia can be understood in terms of its plate tectonic setting, at the regional scale seismicity in Australia shows a marked spatial patterning (Fig. 2) consistent with a control associated with lithospheric structure. In the central part of the continent there seems to be some association between seismicity and the pre-existing structure as evident by comparison of epicentral maps and the gravity field (Fig. 2b). While this suggests an important role for structural reactivation, along the margins of the continent the pattern of seismicity is less easily interpreted in terms of reactivation because, at least in some cases, it conspicuously avoids what appears to be favourably oriented, very-large scale structure. For example, in the south-west part of the continent, relatively high levels of seismic activity, including two of the largest earthquakes to have affected the continent since recordings began, reflects failure in response to E–W compression within 50 km of the north-trending Darling Fault. Despite the fact that the Darling Fault has a long-lived history of Palaeozoic and Mesozoic dip-slip movement, accommodating ~15 km of sediment in the Perth Basin (Harris, 1994) with a ~100 mGal gravity anomaly (Figs. 3 and 4), there is no historical record of seismicity along

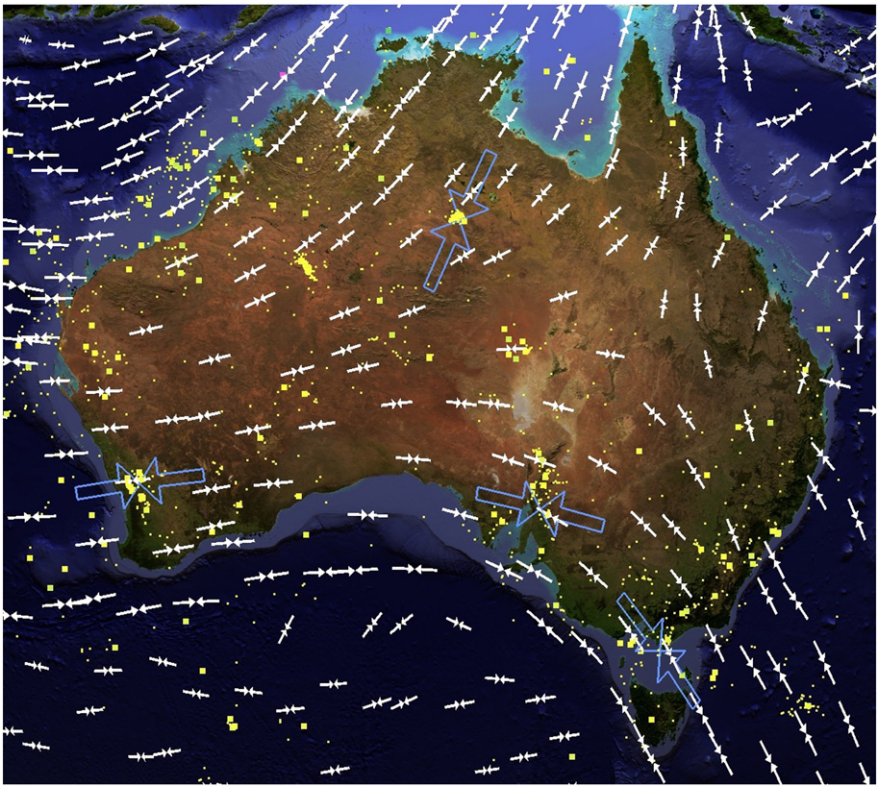

**Fig. 1.** Modelled pattern of stress in the Indo-Australian plate that best fit the *in situ* stress data such as those indicated by selected focal mechanism solutions shown in the large open arrows as well as others (e.g. Hillis and Reynolds, 2000; Reynolds et al., 2002). Earthquake epicentres indicated by yellow dots. Modelling results are based on the plate boundary condition forcings used by Sandiford et al. (2005) adapted from Reynolds et al. (2002). (For interpretation of the references to colour in this figure legend, the reader is referred to the web version of this article.)

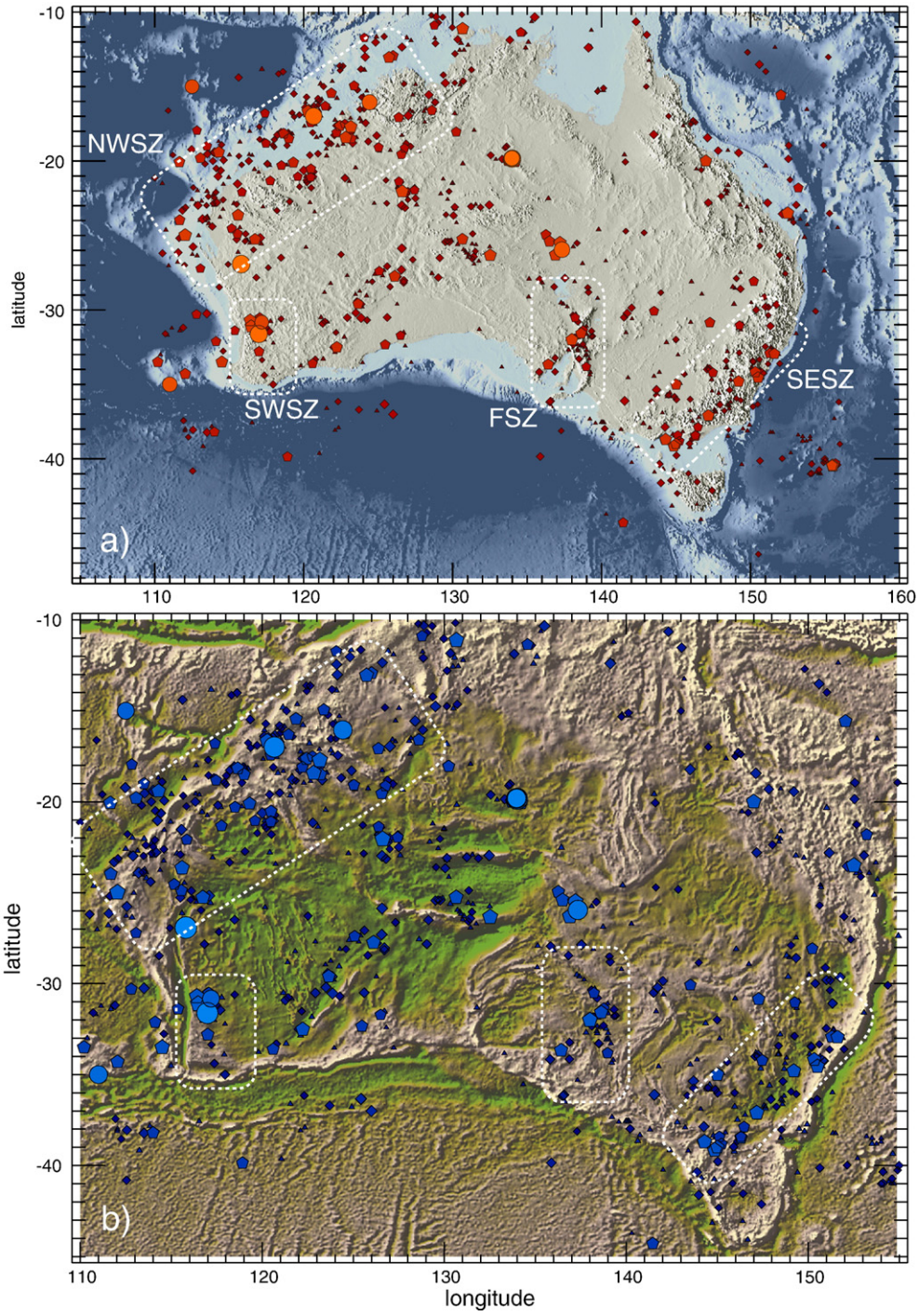


**Fig. 2.** Australian intraplate seismicity overlayed on (a) topography and (b) Bouguer gravity. In the south-east, south-west and north-west the seismicity is concentrated in zones in stretching up to a few hundred kilometres inboard of the ocean–continent transition. Earthquake epicentre data from the geoscience Australia database, with aftershocks removed. Events are shown only for the parts of the catalogue that are considered complete levels (Leonard, 2008) are as follows: $M_L$=3.5–4, 1980+ (triangles), $M_L$=4–5, 1970+ (diamonds), $M_L$=5–5.5, 1960+ and $M_L$=5.5–6, 1910+ (pentagons), $M_L$=6–7, 1910+ (circles) — see Fig. 5. Much of the earthquake activity, but by no means all, occurs in the four seismic zones termed the north-west (NWSZ), south-west (SWSZ), Flinders (FSZ) and south-east (SESZ) seismic zones.

it, nor any indication of Neogene movement. The Darling Fault is a steep (~70°), north-trending structure oriented at 90° to the $S_{Hmax}$. As such it is only miss-oriented with respect to optimal orientation for failure in reverse fault mode by a few 10s of degrees.

In this contribution we explore some factors that may influence mechanical strength of the lithosphere, and hence the variability in the seismic moment release rate, within the Australian continent. We specifically focus on the apparent elevated seismic activity rates along a number of the continent margins (Fig. 2). This distribution suggests that the continent–ocean transition may provide an important control on SCR seismicity, with attendant implications for understanding the reactivation potential of continental structures. As elaborated in more detail below, the continental margin around much of the Australian continent is characterised by significant steps in lithospheric thickness, particularly along the western margin where thick cratonic lithosphere is juxtaposed with Mesozoic oceanic lithosphere and, locally, thinner transitional crust. We explore the effect of lithospheric marginal structure on the pattern of strength distribution in the

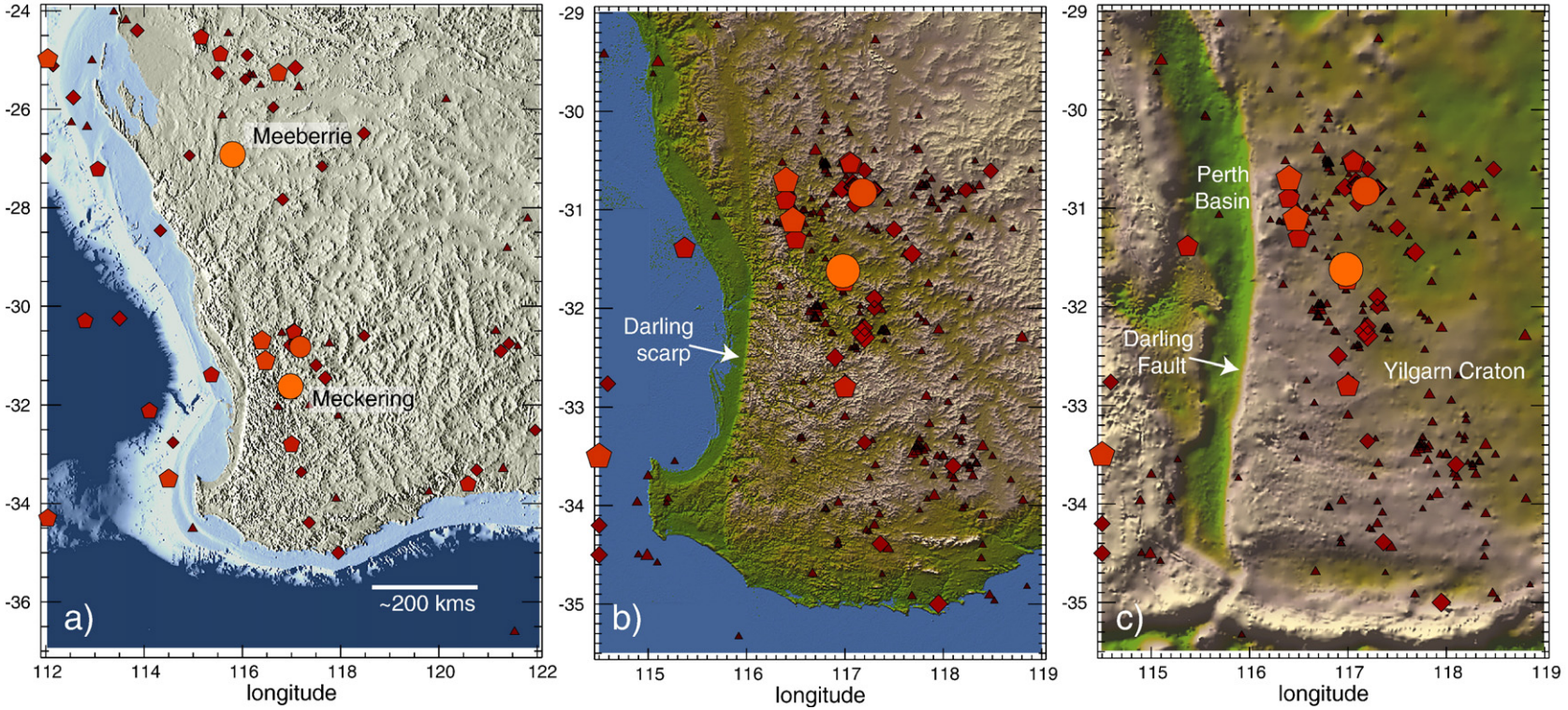


**Fig. 3.** Details of seismicity in the south-west seismic zone, Western Australia. Triangles: a) $M_L$=3.5–4, b) 2.5–4, Diamonds: $M_L$=4–5, Pentagons: $M_L$=5–6, Circles: $M_L$=6–7. In a) the completeness durations as shown in Figs. 2 and 5 are used, while b) and c) show all recorded events since 1910 overlayed on the shaded SRTM-3 arcsecond topography and Bouguer gravity (from Geoscience Australia), respectively. The Bouguer gravity beneath the Perth Basin to the west of the Darling Fault is ~100 mGal lower than the western Yilgarn Craton high. The band of seismicity defining the south-west seismic zone occurs inboard of the continental slope by ~200 km and importantly shows no coincidence with the Darling Scarp/Fault, a major long-lived tectonic feature of suitable orientation for the prevailing E–W $S_{HMax}$ trend (see text for further discussion).

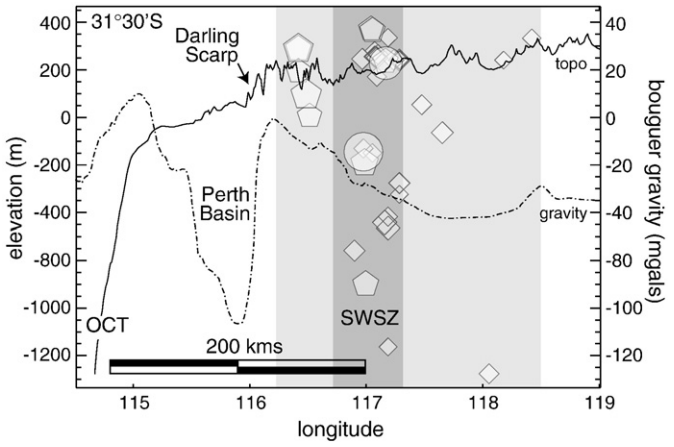


**Fig. 4.** Details of Bouguer gravity (mGal) and topography (m) across the south-western margin of the Australian continent including the SWSZ (shaded zone) in western Australia. The longitudinal profile line is at 31°30′S at approximately the latitude of the $M_w$ 6.6 Meckering earthquake indicated by the central circle. Other major earthquakes are also indicated projected in map view onto the image plane, with North-up (see Fig. 3 for details).

adjacent continent using insights obtained from lithospheric-scale thermal and mechanical models. We begin with a brief summary of the historical pattern of seismicity within Australia.

## 2. Distribution of Australian intraplate seismicity

As with all SCR regions it is important to recognise the impact of catalogue completeness when characterising spatial variations in seismic activity. For Australia, the issue of catalogue completeness has recently been reviewed by Leonard (2008), to which the reader is referred for further information. Fig. 2 shows the inventory of Australian seismic activity that allows for assessment of catalogue completeness as described by Leonard (2008). Fig. 5 shows recorded epicentres of recent Australian earthquakes of magnitude greater than 3.5, for the durations for which the catalogue is considered complete (Leonard, 2008). Spatial variability in earthquake occurrence is apparent. For example, there is enhanced seismic activity along a number of the continental margins — and indeed to first order the map outline of the continent is imaged by the distribution of seismicity, albeit rather vaguely in some regions. While a number of the largest events, such as the 1988 $M_w$ 6.6 Tennant Creek quake of 1988, have occurred in hitherto seismically quite regions, it is now recognised that a significant proportion of Australian seismicity is concentrated into a several distinct seismic zones (Fig. 2; Leonard, (2008). In south-east Australia seismic activity defines a belt (SESZ) that trends parallel to the east coast from central eastern New South Wales south through eastern Victoria into Tasmania. Similarly, the Flinders seismic zone (FSZ) is a zone of relatively enhanced seismic activity centred on the Flinders Ranges in South Australia, corresponding in large part to the Palaeozoic Adelaide fold belt, itself representing the inversion axis of an older Neoproterozoic rift basin (Jenkins and Sandiford, 1992; Paul et al., 1999). The south-west seismic zone (SWSZ — Dentith and Featherstone, 2003) is a N- to NNW-trending belt of elevated seismicity around 100 km inland from Perth, that includes the 1968 $M_w$ 6.7 Meckering event. At the regional scale, the SWSZ lies on a trend that projects northwards along the Western Australian margin to Meeberrie (Fig. 2), the site of Australia's largest onshore earthquake in historical times ($M_w$ ~6.8, 1941). Further north, the most seismically-active part of the Australian continent is located along the north-west shelf (NWSZ).

As noted in the Introduction, the relationship between the distribution of seismicity and crustal and lithospheric structure in Australia is unclear, resulting in significant uncertainty over what controls the distribution of earthquake activity. For example, the NE-trending zone of seismic activity containing the largest earthquakes in the SESZ (Spassov et al., 1997) is clearly oblique to NNW- to N-trending crustal tectonic fabric acquired during Palaeozoic accretion along the eastern seaboard of Gondwana. *In situ* stress indicators (Hillis and Reynolds, 2000; Reynolds et al., 2002) and plate scale stress modelling (Coblentz et al., 1995, 1998; Sandiford et al., 2004b) show the prevailing $S_{Hmax}$ orientation trends south-east at a high angle to the coast (Fig. 1), suggesting a lithospheric-scale process related to the structure of the continental margins may provide an important control (e.g. Spassov et al., 1997; Spassov and Kennett, 2000). Indeed, the central part of the SESZ corresponds to a zone of relatively thick crust, with Moho depths estimated at up to 50 km beneath the Great Dividing Range in south-eastern New South Wales and eastern Victoria (Clitheroe et al., 2000). In the FSZ, there is a clear spatial link between inherited Palaeozoic structure. However, the distribution of seismicity also shows a marked coincidence with a regional heat-flow anomaly (Neumann et al., 2000), and thus the extent to which seismicity is localised by crustal structures or lithospheric-scale variations in thermal state is unclear (Celerier et al., 2005; Quigley et al., 2006).

In the SWSZ, Dentith and Featherstone (2003) have shown that the distribution of seismicity coincides with local structure evident in the seismic profiles. However, at the regional scale, the absence of seismicity on the Darling Scarp is striking (Fig. 3), since this is clearly the most prominent crustal-scale structure evident in its gravity field (Fig. 3c). The Darling Fault (Fig. 3c) is a ~1000 km long, ~70° west-dipping, north-trending structure that coincides with the Darling scarp for much of its length (Harris, 1994; Veevers, 2000). It is set about 80 km inboard of the edge of the continental shelf, and shows repeated reactivation in the Palaeozoic and Mesozoic (Harris, 1994; Veevers, 2000) between the Yilgarn Craton to the east from the Perth Basin to the west. The pronounced ~100 mGal gravity low over the Perth Basin (Figs. 3c and 4) reflects thick accumulations (up to 15 km) of Palaeozoic and Mesozoic sediment above transitional crust between the craton and the ocean (Harris, 1994). As noted above, despite the fact that it is reasonably favourably oriented to accommodate movement in the contemporary stress field (Fig. 1), there is no historical record of seismicity of documented evidence for Neogene movement on the Darling Fault. Understanding why the Darling Fault remains inactive despite relatively high levels of earthquake activity in the adjacent SWSZ remains a major challenge in providing a cogent account of intraplate seismicity in Australia, with implications for global SCR seismicity.

An intriguing aspect of the NW-, SW- and SESZs, relates to the confinement of most intense activity to a ~200 km wide belt that

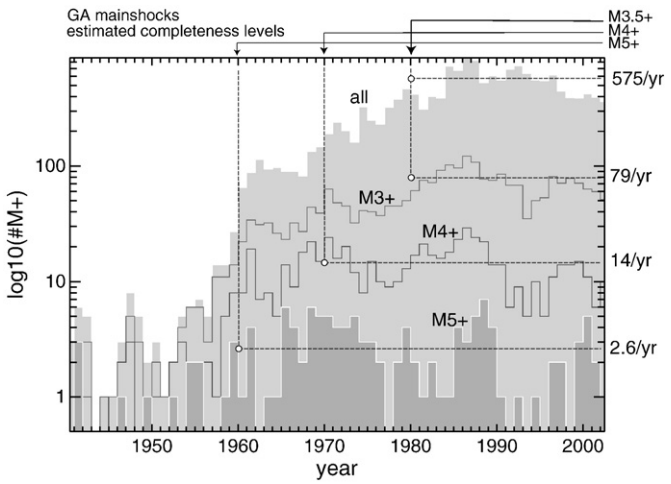


**Fig. 5.** Catalogue completeness inventory for the Geoscience Australia database, after Leonard (2008). The database has been screened to remove aftershocks.

parallel's to the margin. In the SESZ and SWSZ, the continent–ocean transition lies at a high angle to the $S_{Hmax}$ azimuth, and the peak in the seismic moment release is located within the continent rather than on the continental shelf. As such, seismic activity cannot be entirely attributed to reactivation of specific structures created during the development of the continental margin — a point that is dramatically illustrated by the absence of seismicity along the Darling Scarp in the SWSZ. The more highly 'stressed' and seismically-active SW and SE margins of the continent can be compared to the southern margin which parallels the trend and $S_{Hmax}$ and has a much lower level of seismic activity with no coherent spatial link between the margin and seismicity (Figs. 1 and 2). The NWSZ shows a maximum moment release on the continental shelf, perhaps reflecting the much broader shelf, characterised by laterally extensive passive margin sedimentary accumulations, at least compared to the south-eastern and south-western Australian margins. However, even in the NWSZ there is significant elevated moment release onshore, beyond the realm of the rifted margin implying, that reactivation of rift-related structures cannot account for all contemporary seismic activity.

In addition to the development of sets of linked faults within the crust and upper mantle that should facilitate subsequent structural reactivation, rifted passive margins are likely to be characterised by a larger-scale mechanical structuring stemming from the thermal and compositional structuring of the transitional lithosphere. For example, the Western Australia margin juxtaposes thick cratonic continental lithosphere against much thinner oceanic lithosphere with implied steep gradients in lithospheric thickness across the seismically-active margins (see later discussion). Our purpose here is to show just how the thermal and compositional structuring of continental margins subject to gradients in lithospheric and crustal thickness might effect the mechanical response at lithospheric scales, appropriate to understanding variations in seismic activity at wavelengths of order 100 km, and whether we can use the 'marginal' seismicity in the Australian continent to better inform our understanding of the controls on the rheological character of the continents.

## 3. Thermal and mechanical structure of continental margins

As we have suggested above, the spatial link between several of Australia's most active earthquake zones and continental margins suggests that the large-scale structure of the margins may provide an important clue to understanding Australia's seismic moment distribution. To the extent that there is no clear correlation between the distribution of seismicity in these zones and the upper crustal structure, we are motivated to explore the extent to which the passive margin structure at the lithospheric scale may impact on strength distributions, following the insights of Steckler and ten Brink (1986). Because one of the most important factors in determining bulk 'static' strength of the lithosphere is its thermal state we begin by focussing on the thermal structure of the continental margin and then use numerical models to explore whether thermal structuring of continental margins can lead to systematic spatial patterning of strength distributions across passive margins, in a way consistent with the seismic record of Australia's stressed margins.

### 3.1. Lithospheric-scale thermal structure of passive margins

Once the thermal transients associated with opening of marginal ocean basins are dissipated, the thermal structure of passive margins can be understood in terms of steady state heat conduction. Gradients in crustal and lithospheric thickness across the margin necessarily lead to lateral heat flow. At shallow levels, continents are generally hotter than adjacent oceans because of the relatively high near-surface heat production in the upper part of the continental crust. As a consequence, the upper parts of the marginal continental crust will tend to 'bleed' heat into adjacent ocean, inducing cooling of the marginal continental crust with respect to more distal continental interiors (Fig. 6). Contrawise, in the deep parts of the lithosphere, oceans will be hotter than adjacent continental lithosphere if there is any increase in lithospheric thickness across the ocean–continent transition (OCT). Steps in lithospheric thickness across margins will thus induce lateral heat flow directed towards the continents, tending to heat the marginal parts of the continent relative to the more distal continental interior. Thus the relative thermal state of marginal continental crust will be dictated by two distinct, competing lateral heat transfer mechanisms, and whether the marginal continental lithosphere is hotter or cooler than more distal interior parts of the continents will depend primarily on whether the lithosphere thickens beneath the passive margin. Further modification of the marginal crustal thermal structure is possible if they are characterised by thick sedimentary basins with thermal properties distinct from the bulk crust such as conductivity (e.g. Sandiford, 1999).

To illustrate how lithospheric thickness variations impact on the thermal structure of an old passive margin we adopt a simple model appropriate to a thermally-evolved structure in which the thermal transients associated with rifting and ocean lithosphere creation have essentially decayed (i.e., more than 60 myr has passed since sea floor spreading). Because the relevant Australian margins are largely starved of sediment we begin by ignoring the role of sedimentation, although in effect this amounts to considering a virtual sediment wedge that is indistinguishable from the continental upper crust in terms of its thermal properties such as thermal conductivity and heat production. In our models, the OCT is characterised by an increase in thickness of the crust from 7 km beneath the ocean to 28–45 km beneath the continent (Fig. 6). We consider an ocean lithosphere 100 km thick appropriate to old ocean floor (>60 myr) and allow the thickness in continental lithosphere to vary. In the continent interior crustal thickness is ~25% of the total lithosphere thickness, and to maintain local isostatic balance, crustal thickness is varied with lithospheric thickness so as to keep surface elevation at a constant level relative to the ocean floor. The form of the step in Moho and lithospheric thickness is described analytically in terms of an error function:

$$L(x) = L_0 + \frac{\Delta A}{2}\left(1 + \mathrm{erf}\left(\frac{x - x_0}{\Delta x}\right)\right)$$

where $L$ is lithosphere thickness, $\Delta A$ is the size of the lithospheric step, $x$ is the horizontal dimension and $\Delta x$ is a shape factor that's describes the characteristic horizontal scale of the thickness variations. $L_0$ is the thickness of the ocean lithosphere.

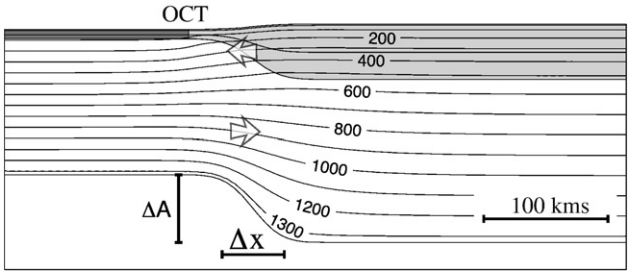


**Fig. 6.** Model set up used in Monte-Carlo simulations. The two variables $\Delta A$ and $\Delta x$ describe the form of the lithospheric step. The ocean–continent transition (OCT) is shown by the boundary between the dark- and light-grey shaded crust. An important feature of continental geotherms is that in the shallow realm they tend to be steeper than oceanic geotherms, while in the deeper realm they are shallower. Because the upper parts of the continental lithosphere tends to be hotter than adjacent ocean lithosphere, shallow level lateral heat flow draws heat away from the continental margin as illustrated by the arrow. In the deeper parts of the continental lithosphere where temperatures tend to be cooler than beneath the oceans, lateral heat flow towards the continent tends to heat the margin. Our calculations show that the 'transition' depth may occur in the sub-continental mantle or the crust depending largely on the magnitude of the lithospheric step ($\Delta A$).

**Table 2**
Rheological and thermal parameters used in numerical models

| Symbol | | Sediment | Upper crust | Lower crust | Mantle |
|---|---|---|---|---|---|
| $k$ [W/m/K] | Thermal conductivity | 2.0 | 3.0 | 3.0 | 4.0 |
| $E$ [Pa] | Young's modulus | $10^{11}$ | $10^{11}$ | $10^{11}$ | $10^{11}$ |
| $v$ | Poisson's ratio | 0.25 | 0.25 | 0.25 | 0.25 |
| $B$ [MPa $s^{(1/n)}$] | Creep parameter | 208.0 | 208.0 | 12.28 | 0.2628 |
| $N$ | Creep parameter | 3.10 | 3.10 | 3.20 | 4.48 |
| $Q$ [kJ/mol] | Creep parameter | 135 | 135 | 239 | 498 |
| $\rho$ [kg/m$^3$] | Density | 2300 | 2800 | 2900 | 3300 |

Creep parameters $B$, $n$ and $Q$ are from Chopra and Paterson (1981) for mantle (wet dunite), from Shelton and Tullis (1981) for lower crust (anorthosite), and from Paterson and Luan (1990) for upper crust (wet quartzite).

We use a Monte-Carlo approach to show the outcome of 1000 combinations of allowable thermal and structural parameters following the methods outlined in (Hansen and Nielsen, 2002; Sandiford et al., 2004a). We characterise the thermal structure of the continent in terms of the position of the Moho temperature maxima, and the temperature difference, $\Delta T$, between the maximum modelled Moho temperature and the reference continental Moho temperature $T_{center}$ ($\Delta T = T_{max} - T_{center}$). The reference Moho temperature of the continental interior, $T_{center}$, is effectively set by the Moho temperature along the right hand end of the model domain, and is typically around 520 °C (relative to a surface temperature of 0 °C). $\Delta T$ is necessarily either zero, for models with maximum Moho temperature along the right hand model boundary, or greater than zero for models that show maximum Moho temperature within the model domain in the vicinity of the OCT. The modelled domain is 500 km long, with a 350 km distance from the OCT to the continental 'interior' boundary. Thermal conductivities are listed in Table 2, and crustal heat production ($H(z) = 3.0 \times 10^{-6} \exp(-z/10\ \text{km})$ ) is assumed to be a function of burial depth in the unstretched lithosphere (see Appendix). The oceanic crust is assumed free of heat production. The lithospheric step gradient is allowed to vary in the parameter range: 0 km $< \Delta A <$ 70 km and 20 km $< \Delta x <$ 70 km. Thermal parameters such as conductivity and crustal heat production are outlined in Table 2. Results of the Monte-Carlo simulation are summarised in Fig. 7.

Fig. 7a shows that ~70% of our model runs result in $\Delta T$ greater than 0, with the maximum Moho temperature occurring along the continental margin at between 100 and 200 km inboard of the OCT. The remaining 30% of parameter sets, that show a temperature maxima in the continental interior are all characterised by lithospheric steps ($\Delta A$) below 30 km (Fig. 7b). For all models with steps less than about 25 km, $\Delta T$ is zero, independently of any other parameter combination. Thus our analysis suggests the single most important factor in determining whether the margin is hotter than the continental interior is the size of the lithospheric step. Providing the lithospheric step is greater than 50 km, the Moho beneath the margin will be up to 35 °C hotter than beneath the continental interior, with a median $\Delta T$ of ~12 °C for all runs with $\Delta A > 50$ km. Large values of $\Delta T$ are restricted to low values of $\Delta x$ (Fig. 7d), and there is a systematic increase in $X_{Tmax}$ with increasing $\Delta x$ (Fig. 7d–e).

### 3.2. Thermo-mechanical structure of passive margins

The temperature dependence of lithospheric rheology implicit in most rheological models of lithospheric deformation imply that the various thermal scenarios revealed by our Monte-Carlo simulation

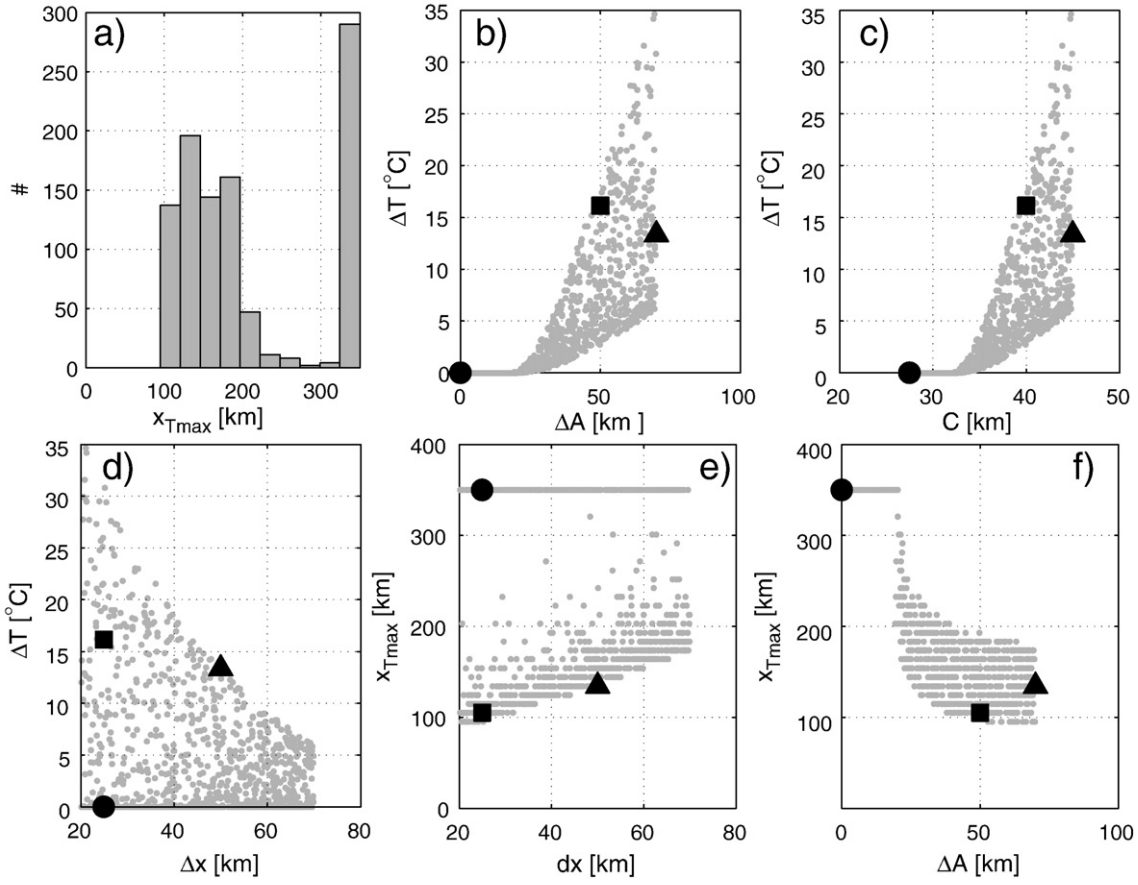


**Fig. 7.** Results of Monte-Carlo simulations with relative Moho temperature difference $\Delta T = T_{max} - T_{center}$ as a function of $\Delta A$, $C$ (continental crustal thickness) and $\Delta x$. $\Delta T$ is the difference between maximum Moho temperature and the continental interior Moho temperature. $x_{Tmax}$ is the distance from the OCT of the maximum Moho temperature. The models for which results shown in Fig. 8 are highlighted using three symbols; the circle is the 'flat-base' model (Models 1 and 4, $\Delta A = 0$ km and $\Delta x = 20$ km), the square is the 'intermediate-step' model with (Model 2: $\Delta A = 50$ km and $\Delta x = 20$ km), and the triangle is 'big-step' (Model 3: $\Delta A = 70$ km and $\Delta x = 50$ km).

have the potential for rather different mechanical responses to far-field forcing. In order to explore this, we consider explicitly the mechanical response of four distinct lithospheres configured with parameter sets as illustrated by the symbols in Fig. 6c–e. In terms of the parameters $\Delta x$ and $\Delta A$, these models are:

- Model 1: with a flat lithospheric base ($\Delta A$=0 km, $\Delta x$=25 km, Fig. 8a–c; circle in Fig. 7),
- Model 2: with an intermediate-step and steep-Moho gradient ($\Delta A$=50 km, $\Delta x$=25 km, Fig. 8d–f, square in Fig. 7) and
- Model 3: with a big-step, and relatively low-Moho gradient ($\Delta A$=70 km, $\Delta x$=50 km, Fig. 8g–i, triangle in Fig. 7).
- Model 4: as for Model 1 but with a margin sedimented with relatively insulating sediments (Fig. 8j–l).

We model the 2D mechanical response of the lithosphere subject to imposed shortening rates that produce strain rates of order $10^{-16}$ s$^{-1}$, appropriate to intraplate deformation, assuming a mechanical response dictated by a combination of frictional sliding and temperature dependant creep processes. The modellings strategy is adapted from (Hansen et al., 2000), where details of the rheological model and benchmarking are described in detail (see also Appendix). We assume plane-strain deformation, subject to an imposed velocity boundary condition, with initial steady state thermal conditions.

In model M1 the absence of a lithosphere step precludes any lateral flow of heat from sub-ocean lithosphere into the margin. Because maximum Moho temperatures are located in the continental interior (Fig. 8b), there is a broad zone of relatively low intensity deformation (~$10^{-16}$ s$^{-1}$) centred about the continental interior. The margin is characterised by steady ocean-ward decrease in crustal strain rates to ~$10^{-17}$ s$^{-1}$ with the steepest gradients in strain rate at 50–100 km inboard of the OCT, reflecting the fact that the continental lithosphere is significantly weaker than the ocean lithosphere.

In models 2 and 3, the lithospheric step induces significant lateral heat flow, heating the lithosphere beneath the margin relative to the interior, such that maximum Moho temperatures at any depth are located at around 20–50 km inboard of the OCT (Fig. 8e and h). The position of maximum Moho temperature is dependant on the parameter $\Delta x$, being further inboard for Model 3 than Model 2 because of the shallower Moho depth gradients in the former. A peak in the maximum crustal strain rates occurs along the Moho, essentially coinciding in space to the peak in Moho temperatures at around 75 and 100 km inboard of the OCT for Model 2 and Model 3, respectively. Maximum strain rates are an order of magnitude higher than those beneath the OCT and up to 3 times greater than for the continental interior. Fig. 8d and g show that the locus of maximum deformation is shifted continent-ward at shallower crustal depths, so

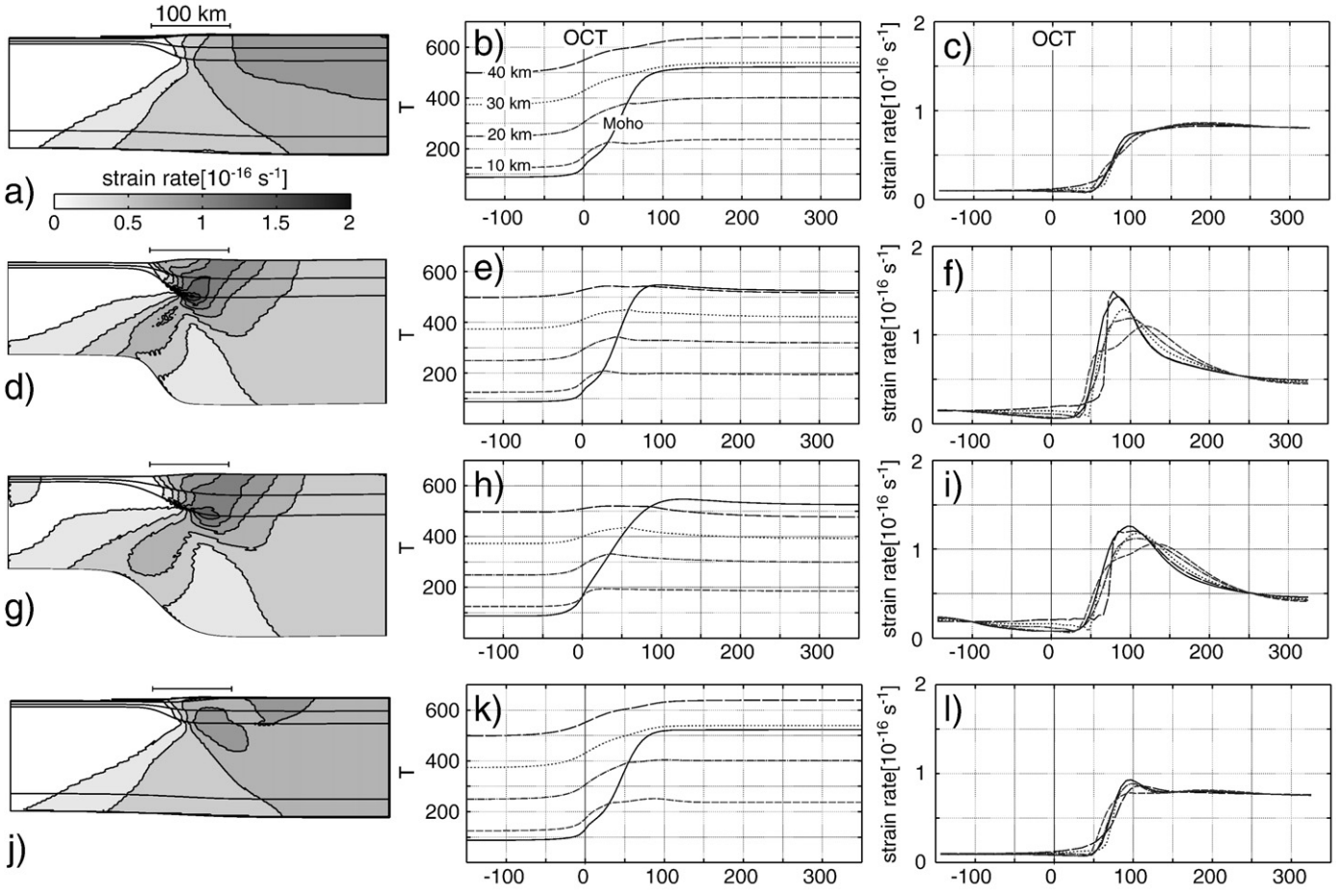


**Fig. 8.** Strain-rate distributions for the four representative lithospheric models discussed in the text. For the strain-rate measure the square root of the second invariant of the bulk (elastic+plastic+viscous) strain-rate tensor is used. (a–c) model M1 : $\Delta A$=0 km and $\Delta x$=20 km, (d–f) Model M2: $\Delta A$=50 km and $\Delta x$=20 km, (g–i) model M3: $\Delta A$ =70 km and $\Delta x$=50 km, and (j–l) model M4: as for M1 but with insulating sedimentary prism. The left column shows lithospheric sections contoured for strain rate. The central column shows temperature profiles at 10, 20, 30 and 40 km depth and at the Moho (solid line) as a function of distance (in km) from the ocean–continent transition (OCT). The right column shows strain-rate profiles at the depths corresponding to those shown in the temperature profiles as a function of distance (in km) from the OCT. Magnitudes of deviatoric stresses increase linearly with depth in the upper part of the upper crust (which is brittle) reaching levels of ~200 MPa. Deviatoric stress increases across the mineralogical boundaries (upper–lower crust and crust–mantle) but decreases with depth as here deformation is ductile and temperature dependent. The highest deviatoric stress (~500 MPa) is in the upper mantle just below the crust–mantle transition.

that in the shallow seismogenic parts of the crust the deformation locus is 100 and 150 km inboard of the OCT for both models (see also Fig. 8f and i).

Fig. 8j–l shows the results of Model 4 designed to illustrate the effects of a insulating sedimentary cover in a model otherwise equivalent to Model 1 (i.e., Fig. 8a–c). To do so we impose a sedimentary prism on the margin, that attains a maximum thickness of 4 km, with a thermal conductivity of 2 W/m/K. The insulating properties of the sedimentary prism lead to some heating of the lithosphere beneath the margin, and a relatively slight shift in the locus of deformation from the margin to the interior. However, the impact of the insulating cover is relatively minor, reflecting that the associated thermal 'loading' of the critical, mechanically-sensitive part of the lithosphere is subordinate to the thermal loads stemming from deep lithospheric structure.

Application of our modelling to specific settings requires interpretation because of the idealised geometry we have used, in which crust and lithospheric thickness variations are modelled with the same error-function dependence on distance from the OCT. There are no observations that justify the use of such a simple analytic model, and it is used here only because of its utility as a parameterisation in terms of just two parameters $\Delta x$ and $\Delta A$. In reality, passive margins are likely to have complicated structure and the precise form of crustal and lithospheric thickness variations will be more complex. Arguably the salient point of our models is that, in presence of significant lithospheric steps, lateral heat flow will contribute heating of the Moho within a distance of order of 100 km inboard of the step. Maximum Moho temperatures, and strength distributions, will be dependant on the precise disposition of crustal thickness and lithospheric thickness variations across the margin, and the distance measure from the OCT that we have used in our models should be interpreted more generally as the distance from the outboard side of any effective lithospheric step beneath a margin. Our models show shallow seismogenic deformation induced by this thermal structuring is localised marginally inboard of the transition to full thickness continent crust, in regions that are consequently unaffected by the structures that effected thinning of the crust along the passive margin. Of course our models do not specifically incorporate weakening effect of such "passive margin" structure, which could conceivably impact on the distribution of strain, as we have shown is possible in a minor way for sediment loaded margins. We return to this question of the role of structural reactivation with specific reference to the Darling Fault in the subsequent below.

## 4. Seismic velocity constraints on lithospheric structure

The calculations summarised in this contribution illustrate that the thermal and compositional structuring of continental margins has the potential to produce significant mechanical structuring. Providing the continental thermal lithosphere is more than about 30 km thicker than the adjacent oceanic lithosphere then marginal heating due to lateral heat flow is likely to generate relatively weak margins. In Australia, such conditions are likely to apply around much of the continent, and particularly in the west, where the OCT juxtaposes cratonic lithosphere against Mesozoic ocean lithosphere. Seismological studies show that the cratonic lithosphere extends to depths of ~200 km beneath the Yilgarn craton in the south-western part of the continent as well as beneath the Pilbara craton in the north-west (Reading and Kennett, 2003; Kennett et al., 2004; Fishwick et al., 2005). The western Australian cratonic regions are characterised by very fast shear wavespeeds, with particularly strong gradients in shear wavespeeds along the western boundary of the Yilgarn Craton in the vicinity of the Darling Fault (Kennett et al., 2004). At a depth of 125 km, shear wavespeeds change by ~8% across the Darling Scarp (Kennett et al., 2004; Faul and Jackson, 2005), consistent with temperature differences as much as 500 °C (Fig. 9; Faul and Jackson, 2005). Faul and Jackson (2005) have suggested that the absence of low velocity zone beneath these cratons implies sub-adiabatic temperatures extend into the lower half of the upper mantle, implying a difference in lithospheric thickness in excess of 100 km across the western Australian margin.

As noted earlier, a perplexing aspect of the seismic activity in the SWSZ relates to the lack of activity along the Darling Fault. While the location of the Darling Fault some ~80 km inboard of the edge of the continental shelf might appear to be in prime position to be reactivated, this is probably a rather too literal application of our modelling results. Because the Darling Fault coincides with the strongest gradients in lithospheric and crustal thickness along the margin (e.g. Reading et al., 2003), the prime insight stemming from our modelling is that the greatest weakening, and hence most favourable locus of seismic moment release must be further inboard, within a relatively narrow band within the craton itself where crust is relatively thick but still close enough to the "effective" OCT to experience lateral conductive heating across the lithospheric step

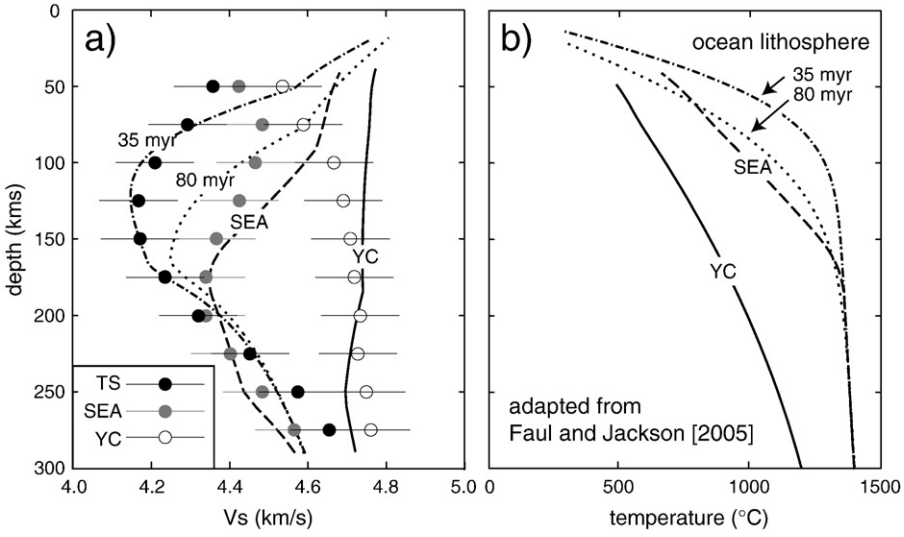


**Fig. 9.** Summary of Australian shear wave velocity data for relevant areas (adapted from Figs. 6 and 7 in Faul and Jackson, 2005). Faul and Jackson (2005) obtained shear wave velocities from the tomographic model of Fishwick et al. (2005) with horizontal bars indicating 1-standard deviation. TS is the central Tasman Sea (ocean lithosphere), SEA is south-east Australia and YC is the Yilgarn Craton. The line profiles correspond to calculated shear wave velocities for 35 myr and 80 myr ocean lithosphere, and to SEA and YC using the geotherms shown in b, and the empirical velocity-temperature conversion of Faul and Jackson (2005). See Faul and Jackson (2005) for further discussion.

beneath the Darling Fault. In our models the "effective" OCT is on the outboard side of the main lithospheric step, which is likely to be directly beneath the Darling Fault. Thus, our modelling results suggests that the absence of seismicity on the Darling Faults may simply reflect the dominant control on deformation being provided by the lithospheric-scale thermal structuring of the margin. A corollary, discussed further in the next section, is that the reactivation potential of the Darling Fault is subordinate to thermal controls on lithospheric strength induced by lateral heat transfer across the margin.

Gradients in lithospheric and crustal thickness across the north-west margin appear to rather more gentle than along the edge of the Yilgarn Craton in the south-west, and the relatively broad zone of seismicity here may reflect both the effects of a larger effective $\Delta x$, and the impact of a much thicker passive margin sedimentary cover, locally in excess of 6 km thick (Veevers, 2000).

In contrast with the western Australian margin, shear wavespeeds in the 75–150 km depth range beneath the south-eastern part of the continent (Fishwick et al., 2005) are comparable with the shear wavespeeds expected for old ocean lithosphere (e.g. Faul and Jackson, 2005, Fig. 9a) and it seems unlikely that there is significant step in the thermal lithospheric thickness across this margin. One potential lithospheric control that may help play a role in weakening the lithosphere in the SESZ is the relative deep Moho beneath the Snowy Mountains (Clitheroe et al., 2000), reflecting the possibility that both lithospheric and crustal thickness gradients are important in controlling the distribution of deformation along stressed margins.

## 5. The role of "structural reactivation"

The structural geological literature is replete with appeals to structural reactivation in continental interiors and mountain belts, to the extent that pre-existing structures are often assumed to play the primary role in localising subsequent deformation. At one level, the ability of faults such as the Darling Fault to accumulate ongoing slip, and hence reactivate, is self-evident. Reactivation is clearly needed by the requirement to accommodate large movement, and demanded by many instances in the geological record. However, the way in which such structures continue to impact on long-term behaviour of continents in regimes in which the intraplate stress field evolves in response to far-field factors such as changes plate tectonic palaeo-geography is far from clear (e.g. Holdsworth et al., 1997; Butler et al., 2006). While there are clearly many studies that demonstrate structural reactivation plays an important role in the tectonic evolution of the continents, there has been far less attention paid to cases where reactivation of apparently suitably-oriented, large-scale structure does not occur. However, such cases hold important clues relevant to better understanding of lithospheric rheology. In part, the potential for reactivation of the Darling Fault must be limited because it is not optimally oriented in an Andersonian sense to accommodate slip in a reverse fault stress field (Sibson, 1985; Etheridge, 1986), being ~30° too steep. However, if the Darling Fault comprises an anastomosing and splayed network of fault strands at depth, as would seem likely given its complex, long-lived history and large displacement, at least some strands are likely to be near optimally oriented with respect to the *in situ* stress field. Such considerations make the total absence of seismic activity along the Darling Fault surprising, especially in view of the relatively intense seismic activity immediately inboard of the fault in the SWSZ. Here we have suggested an additional mechanism related to thermal structuring that provides a framework for understanding the variability in the distribution of seismicity in south-western Australia at spatial scales of ~100 km, and while our models do not explicitly address the inherent strength of the Darling Fault system, they do place constraints on the relativities of thermal and structural controls on lithospheric strength along the south-western margin. The implication of our analysis is that mechanical consequence of elevating temperatures by 10–30 °C, overwhelms the ability of the Darling Fault to localise failure in the present-day stress field (characterised by E–W $S_{Hmax}$). Intriguingly there appears to be a rather better correspondence between lithospheric structure as revealed by Bouguer gravity field and seismicity within the continent interior than along the margin (Fig. 2b). This suggests that the strength character of continents is a mosaic dictated by complex thermal and structural parameters. While this conclusion is hardly novel, the importance of our work is that it provides a clue as to the relative small magnitude of thermal structuring (order 10°) needed to suppress structural reactivation of near optimally oriented structure.

The notion that thermal processes might provide an important "switch" controlling fault reactivation has been postulated for other settings. For example, the selective reactivation of faults during Palaeozoic Central Australian Basins has been attributed to thermal causes related to long-term changing patterns of sedimentation (Sandiford and Hand, 1998; Hand and Sandiford, 1999). At a larger scale (Neil and Houseman, 1997) have argued that deformation partitioning across central Asia, between the Tarim Basin and Tian Shan, could be explained by Moho Temperature variations of 10–30 °C. Similarly seismic activity in the New Madrid zone in an intraplate setting analogous to Australia has been attributed to thermal process evident in a surface heat-flow anomaly of about 15 mW $m^{-2}$ (Liu and Zoback, 1997), that would be expressed as a Moho temperature rise of a few tens of degrees. In Australia, Celerier et al. (2005) have appealed to heat-flow variations to explain seismicity in the FSZ. Implicit in these models is the notion of extreme temperature dependence of lithospheric rheology, largely derived from extrapolation of experimentally derived flow laws (e.g. Brace and Kohlstedt, 1980; Ord and Hobbs, 1989) but consistent with the very strong temperature dependence required to explain the dynamics of the mantle's interior convective engine. There has been a long history of trying to establish meaningful constraints on lithospheric rheology on the basis of geological observables (e.g. Sonder and England, 1986; England, 1987; Zoback et al., 2002), but this continues to prove contentious. We suggest that the relative roles of structural and thermal processes in controlling the distribution of seismicity around the Australian continental margin provides one such set of observations relevant to the assessment of the temperature dependence of lithospheric rheology.

## 6. Further implications

The hypothesis that the thermal structuring of continental margins provides a long-term control on the distribution of subsequent deformation along continental margins in intraplate settings may help solve some other perplexing attributes of continental evolution, such as the formation of long ribbon like micro-continental fragments and slivers such as the Lord Howe and New Caledonia Rises, off the east coast of Australia. These "ribbon" like fragments of continent are characterised by relatively uniform across strike width of a few hundred km extending along strike for 1000 km or more. While there are only a few examples on the modern earth, "ribbon" continents of the ilk of the Lord Howe Rise have been inferred in many ancient orogenic systems (e.g. Muller et al., 2001; von Raumer et al., 2003; Cawood et al., 2007), where they help explain complex polyphase accretion histories. Thus, while continental ribbons seem to have been a relatively common outcome of repeated rifting of passive continental margins in the geological record, there has been little understanding of the mechanics of their formation. Such features require a mechanical structuring of continental margins that is analogous to that proposed for Australian intraplate seismicity here — namely, a process that localises failure ~100–200 km inboard of the OCT.

## 7. Main conclusions

[1] Numerical simulations show that thermal structuring associated with lateral heat flow induced by steps in lithospheric and crustal thickness along continental margins can lead to significant mechanical weakening with respect to continental interiors.

[2] Applications of this modelling to the seismically-active western margin of the Australian continent, may help explain why structures such as the Darling Fault remain inactive in spite of significant seismic activity only a few 10s of km further inboard.
[3] Temperature variations of a few 10s of degrees at Moho depths provide sufficient mechanical strength variations at the lithospheric scale to overwhelm structural reactivation.

## Acknowledgments

This work has been supported by ARC Discovery grants DP0558705 and DP556133. Mark Leonard is thanked for providing access to the Geoscience Australia database. We thank Dan Clark for discussion and comments concerning the role of continental margin seismicity, and Taras Gerya and Mark Zoback for their reviews. An insightful discussion with Ed Sobel highlighted the potential link to continental ribbon formation.

## Appendix A

Here we outline the background to the thermo-mechanical modelling which is largely based on the recipe of Braun and Beaumont (1987). The two-dimensional thermo-mechanical model is founded on the mechanical equilibrium equations (Malvern, 1969):

$$\frac{\partial \sigma_{ij}}{\partial x_j} + \rho g_i = 0$$

which are solved numerically using a Lagrangian finite-element formulation (Zienkiewicz, 1971) with 9400 isoparametric triangular elements. $\sigma_{ij}$ is the Cauchy stress tensor, $\rho$ is density, $g_i$ is acceleration due to gravity and $x_i$ are the spatial coordinates.

The mechanical equilibrium equations are complemented by a set of constitutive relations enabling visco-elastic and plastic deformation. The visco-elastic deformation form simulates temperature and time dependent ductile creep of solid rock mass and is based on a Maxwell relation stating additivity of elastic and viscous strain rates (Jaeger and Cook, 1969). While the elastic strain rates satisfy Hooke's law (Ranalli, 1995) with Young's modulus at $10^{11}$ Pa and Poisson's ratio at 0.25, the viscous strain rates satisfy the empirical Dorn equation, relating effective strain rates and stress levels for steady state creep. In this case, the effective viscosity, $\eta$, is:

$$\eta = B \cdot \varepsilon^{1/n-1} \exp\left(\frac{Q}{nRT}\right)$$

where $\varepsilon$ is effective visco-elastic strain rate, $T$ is absolute temperature, and $R$=8.31 J/(mol K) is the ideal gas constant. $n$, $Q$ and $B$ are experimentally derived creep parameters (Chopra and Paterson, 1981; Shelton and Tullis, 1981) assumed only to depend on mineralogy. The lithospheric section consists of three different mineralogical layers of upper crust (wet quartzite), lower crust (wet anorthosite) and mantle (wet dunite) (see Table 2).

When the yield stress of rocks is reached, the deformation mode becomes visco-elastic–plastic simulating brittle failure. The yield stress is derived from the pressure dependent Griffith criterion (Jaeger and Cook, 1969):

$$F = J_2 + 12 T_0 P$$

where $J_2$ is the 2nd invariant of the deviatoric stress tensor, $T_0$ is tensile strength, and $P$ is lithostatic pressure. The driving, non-lithostatic stresses are assumed not to contribute substantially to the pressure, in which case the associative plastic flow law:

$$\dot{\varepsilon}_{ij}^{p} = \alpha \frac{\partial F}{\partial s_{ij}} \quad \text{for} \quad F>0$$

becomes non-dilatational (Braun and Beaumont, 1987). $\dot{\varepsilon}_{ij}^{p}$ is the plastic strain-rate tensor, $s_{ij}$ is the deviatoric stress tensor and $\alpha$ is found from the condition:

$$s_{ij} \frac{\partial F}{\partial s_{ij}} = 0$$

This particular plasticity model is well suited only for large-scale tectonics as the associative flow law neglects the detailed localizing behaviour of brittle deformation. Instead, brittle failure is represented by relatively smoothly varying plastic strain rates.

The displacement and temperature fields are coupled through the temperature dependence of viscosity and density. The latter is given by:

$$\rho = \rho_0 (1 - a_v T)$$

where $\rho_0$ is density at 0 °C. $\alpha_v = 3.2 \cdot 10^{-5}$ K$^{-1}$ is the volumetric expansion coefficient and $T$ is Celsius temperature.

The lithospheric section is initially 500 km long and uniformly layered. In this initial model geometry, heat production rates are calculated as a function of burial depth. The mesh geometry is then thinned, without solving the mechanical equilibrium equations, to produce the desired initial passive margin structure. The model is hereafter thermo-mechanically shortened 20 km. Shortening is accomplished by moving the left vertical boundary to the right at the speed of 0.5 km/myr. Flexural isostasy is obtained by imposing buoyancy forces along the horizontal layer boundaries.

## References

Brace, W.F., Kohlstedt, D.L., 1980. Limits on lithospheric strength imposed by laboratory experiments. Journal of Geophysical Research 85, 6248–6252.
Braun, J., Beaumont, C., 1987. Styles of continental rifting: results from dynamic models of lithospheric extension. Memoir of the Canadian Society of Petroleum Geologists 12, 241–258.
Braun, J., Burbidge, D.R., Gesto, F.N., Sandiford, M., Gleadow, A.J.W., Kohn, B.P., Cummins, P.R., in press, Constraints on the current rate of deformation and surface uplift of the Australian continent from a new seismic database and low-T thermochronological data. Australian Journal of Earth Sciences.
Butler, R.W.H., Tavarnelli, E., Grasso, M., 2006. Structural inheritance in mountain belts: an Alpine–Apennine perspective. Journal of Structural Geology 28 (11), 1893–1908.
Cawood, P.A., Johnson, M.R.W., Nemchim, A., 2007. Early Palaeozoic orogenesis along the Indian margin of Gondwana: tectonic response to Gondwana assembly. Earth and Planetary Science Letters 255, 70–84. doi:10.1016/j.epsl.2006.12.006.
Celerier, J., Sandiford, M., Hansen, D.L., Quigley, M., 2005. Modes of active intraplate deformation, Flinders Ranges, Australia. Tectonics 24. doi:10.1029/2004&C001679.
Chopra, P.N., Paterson, M.S., 1981. The experimental deformation of dunite. Tectonophysics 78, 453–473.
Clitheroe, G., Gudmundsson, Ó., Kennett, B.L.N., 2000. The crustal thickness of Australia. Journal of Geophysical Research 105, 13697–13713.
Coblentz, D., Sandiford, M., 1994. Tectonic stress in the African plate: constraints on the ambient stress state. Geology 22, 831–834.
Coblentz, D.D., Sandiford, M., Richardson, R.M., Zhou, S., Hillis, R., 1995. The origins of the intraplate stress field in continental Australia. Earth and Planetary Science Letters 133 (3–4), 299–309.
Coblentz, D.D., Zhou, S., Hillis, R., Richardson, R., Sandiford, M., 1998. Topography, plate-boundary forces and the Indo-Australian intraplate stress field. Journal of Geophysical Research 103, 919–931.
DeMets, C., Gordon, R.G., Royer, J.Y., 2005. Motion between the Indian, Capricorn and Somalian plates since 20 Ma: implications for the timing and magnitude of distributed lithospheric deformation in the equatorial Indian ocean. Geophysical Journal International 161, 445–468.
Dentith, M.C., Featherstone, W.E., 2003. Controls on intra-plate seismicity in south-western Australia. Tectonophysics 376, 167–184.
Deplus, C., 2001. Plate tectonics: Indian Ocean actively deforms. Science 292 (5523), 1850–1851.
England, P.C., 1987. Diffuse continental deformation: length scales, rates and metamorphic evolution. Philosophical Transactions of the Royal Society of London A231, 3–22.
Etheridge, M.A., 1986. On the reactivation of extensional fault systems. Philosophical Transactions of the Royal Society of London, Series A 317, 179–194.
Faul, U.H., Jackson, I., 2005. The seismological signature of temperature and grain size variations in the upper mantle. Earth and Planetary Science Letters 234, 119–134.
Fishwick, S., Kennett, B.L.N., Reading, A., 2005. Contrasts in lithospheric structure within the Australian craton—insights from surface wave tomography. Earth and Planetary Science Letters 231, 163–176.
Hand, M., Sandiford, M., 1999. Intraplate deformation in central Australia, the link between subsidence and fault reactivation. Tectonophysics 305 (1–3), 121–140.

Hansen, D.L., Nielsen, S.B., 2002. Does thermal weakening explain basin inversion? Stochastic modelling of the thermal structure beneath sedimentary basins. Earth and Planetary Science Letters 198, 113–127.
Hansen, D.L., Nielsen, S.B., Lykke-Andersen, H., 2000. The post-Triassic evolution of the Sorgenfrei–Tornquist Zone. Tectonophysics 328, 245–267.
Harris, L.B., 1994. Structural and tectonic synthesis for the Perth Basin, Western Australia. Journal of Petroleum Geology 17, 129–156.
Hillis, R.R., Reynolds, S.D., 2000. The Australian stress map. Journal of the Geological Society London 157, 915–921.
Holdsworth, R.E., Butler, C.A., Roberts, A.M., 1997. The recognition of reactivation during continental deformation. Journal of the Geological Society London 154, 73–78.
Jaeger, J.C., Cook, N.G.W., 1969. Fundamentals of Rock Mechanics. Chapman and Hall Ltd., London.
Jenkins, R.J.F., Sandiford, M., 1992. Observations on the tectonic evolution of the southern Adelaide Fold Belt. Tectonophysics 214 (1–4), 27–36.
Johnston, A.C., Coppersmith, K.J., Kanter, L.R., Cornell, C.A., 1994. The earthquakes of stable continental regions. Electric Power Research Institute Publication TR-102261-V1, Palo Alto, California.
Kennett, B.L.N., Fishwick, S., Heintz, M., 2004. Lithospheric structure in the Australian region — a synthesis of surface wave and body wave studies. Exploration Geophysics 35, 242–250.
Krishna, K.S., Bull, J.M., Scrutton, R.A., 2001. Evidence for multiphase folding of the central Indian Ocean lithosphere. Geology 29, 715–718.
Leonard, M., 2008. One hundred years of earthquake recording in Australia. Bulletin of the Seismological Society of America 98, 1458–1470.
Liu, L., Zoback, M.D., 1997. Lithospheric strength and intraplate seismicity in the New Madrid seismic zone. Tectonics 16, 585–595.
Malvern, L.E., 1969. Introduction to the Mechanics of a Continuous Medium. Prentice-Hall, inc., New Jersey.
Molnar, P., England, P., Martinod, J., 1993. Mantle dynamics, the uplift of the Tibetan plateau, and the Indian monsoon. Reviews of Geophysics 31, 357–396.
Muller, R.D., Gaina, C., Roest, W.R., Hansen, D.L., 2001. A recipe for microcontinent formation. Geology 39, 203–206.
Neil, E.A., Houseman, G.A., 1997. Geodynamics of the Tarim Basin and the Tian Shan. Tectonics 16, 571–584.
Neumann, N., Sandiford, M., Foden, J., 2000. Regional geochemistry and continental heat flow: implications for the origin of the South Australian heat flow anomaly. Earth and Planetary Science Letters 183 (1–2), 107–120.
Ord, A., Hobbs, B., 1989. The strength of the continental crust. Tectonophysics 158, 269–289.
Paterson, M.S., Luan, F.C., 1990. Quartzite rheology under geological conditions. In: Knipe, R.J., Rutter, E.H. (Eds.), Deformation Mechanisms, Rheology and Tectonics. Geological Society London Special Publication, vol. 54, pp. 299–307.
Paul, E., Flottmann, T., Sandiford, M., 1999. Structural geometry and controls on basement-involved deformation in the northern Flinders Ranges, Adelaide Fold Belt, South Australia. Australian Journal of Earth Sciences 46 (3).
Quigley, M., Cupper, M., Sandiford, M., 2006. Quaternary faults of southern Australia: palaeoseismicity, slip rates and origin. Australian Journal of Earth Sciences 53, 285–301.
Ranalli, G., 1995. Rheology of the Earth. Chapman & Hall, London.
Reading, A.M., Kennett, B.L.N., 2003. Lithospheric structure of the Pilbara Craton, Capricorn Orogen and northern Yilgarn Craton, Western Australia, from teleseismic receiver functions. Australian Journal of Earth Sciences 50 (3), 439–445.
Reading, A.M., Kennett, B.L.N., Dentith, M.C., 2003. Seismic structure of the Yilgarn Craton, Western Australia. Australian Journal of Earth Sciences 50, 427–438.
Reynolds, S.D., Coblentz, D.D., Hillis, R.R., 2002. Tectonic forces controlling the regional intraplate stress field in continental Australia: results from new finite-element modelling. Journal of Geophysical Research 107. doi:10.1029/2001JB000408.
Sandiford, M., 1999. Mechanics of basin inversion. Tectonophysics 305 (1–3), 109–120.
Sandiford, M., 2003. Neotectonics of southeastern Australia: linking the Quaternary faulting record with seismicity and *in situ* stress. In: Hillis, R.R., Muller, D. (Eds.), Evolution and Dynamics of the Australian Plate. Geological Society of Australia Special Publication, vol. 22, pp. 101–113.
Sandiford, M., Hand, M., 1998. Controls on the locus of intraplate deformation in central Australia. Earth and Planetary Science Letters 162 (1–4), 97–110.
Sandiford, M., Frederiksen, S., Braun, J., 2004a. The long-term thermal consequences of rifting: implications for basin reactivation. Basin Research 15, 23–43.
Sandiford, M., Wallace, M., Coblentz, D., 2004b. Origin of the *in situ* stress field in south-eastern Australia. Basin Research 16 (3), 325–338.
Sandiford, M., Coblentz, D., Schellart, W.P., 2005. Evaluating slab-plate coupling in the Indo-Australian plate. Geology 33, 113–116.
Shelton, G., Tullis, J., 1981. Experimental flow laws for crustal rocks. EOS 62, 396.
Sibson, R.H., 1985. A note on fault reactivation. Journal of Structural Geology 7 (6), 751–754.
Sonder, L., England, P., 1986. Vertical averages of rheology of the continental lithosphere; relation to thin sheet parameters. Earth and Planetary Science Letters 77, 81–90.
Spassov, E., Kennett, B.L.N., 2000. Stress and faulting in southeast Australia as derived from the strongest earthquakes in the region. Journal of Asian Earth Sciences 18, 17–23.
Spassov, E.N., B.L.N., K., J., W., 1997. Seismic zoning of Southeast Australia. Australian Journal of Earth Sciences 44, 527–534.
Steckler, M.S., ten Brink, U.S., 1986. Lithospheric strength variations as a control on new plate boundaries: examples from the northern Red Sea region. Earth and Planetary Science Letters 79, 120–132.
Veevers, J.J., 2000. Billion-Year Earth History of Australia and neighbours in Gondwanaland. GEMOC Press, Sydney: p. 388.
von Raumer, J.F., Stampfl, G.M., Bussy, F., 2003. Gondwana-derived microcontinents — the constituents of the Variscan and Alpine collisional orogens. Tectonophysics 365, 7–22.
Zienkiewicz, O.C., 1971. The Finite Element Method in Engineering Science. McGraw-Hill, London.
Zoback, M.D., et al., 1999. Seismic hazard at the New Madrid Seismic Zone. Science 285, 663.
Zoback, M.D., Townend, J., Grollimund, B., 2002. Steady-state failure equilibrium and deformation of intraplate lithosphere. International Geology review 44, 383–401.